JOURNAL OF BACTERIOLOGY, Feb. 1995, p. 699–704 Vol. 177, No. 3
0021-9193/95/$04.00+0

Kinetic Analysis by In Vivo ^{31}P Nuclear Magnetic Resonance of Internal P_i during the Uptake of *sn*-Glycerol-3-Phosphate by the *pho* Regulon-Dependent Ugp System and the *glp* Regulon-Dependent GlpT System

KARINA B. XAVIER,[1] MARINA KOSSMANN,[2] HELENA SANTOS,[1] AND WINFRIED BOOS[2]*

Instituto de Tecnologia Química e Biológica, UNL, 2780 Oeiras, Portugal,[1] and Department of Biology, University of Konstanz, D-78434 Konstanz, Germany[2]

Received 9 August 1994/Accepted 28 November 1994

When *sn*-glycerol-3-phosphate (G3P) is taken up exclusively by the *pho* regulon-dependent Ugp transport system, it can be used as the sole source of P_i but not as the sole source of carbon. We had previously suggested that the inability of G3P to be used as a carbon source under these conditions is due to *trans* inhibition of G3P uptake by internal P_i derived from the degradation of G3P (P. Brzoska, M. Rimmele, K. Brzostek, and W. Boos, J. Bacteriol. 176:15–20, 1994). Here, we report ^{31}P nuclear magnetic resonance measurements of intact cells after exposure to G3P as well as to P_i, using different mutants defective in *pst* (high-affinity P_i transport), *ugp* (*pho*-dependent G3P transport), *glpT* (*glp*-dependent G3P transport), and *glpD* (aerobic G3P dehydrogenase). When G3P was transported by the Ugp system and when metabolism of G3P was allowed (*glpD*$^+$), P_i accumulated to about 13 to 19 mM. When G3P was taken up by the GlpT system, the preexisting internal P_i pool (whether low or high) did not change. Both systems were inversly controlled by internal P_i. Whereas the Ugp system was inhibited, the GlpT system was stimulated by elevated internal P_i.

sn-Glycerol-3-phosphate (G3P) can be taken up in *Escherichia coli* by several transport systems. When used as a carbon source, G3P is taken up exclusively by the GlpT transport system (1, 11, 13). This system is part of the *glp* regulon, a number of proteins whose genes are transcribed in response to the presence of glycerol and G3P in the medium and which are geared for the uptake and the metabolism of glycerol, G3P, and glycerol phosphoryl diesters (15). GlpT and all of the other *glp*-encoded proteins are under the control of GlpR, the repressor of the system (14), with G3P as the effective inducer (16). The GlpT transport system can function in two modes. In the exchange mode, G3P is taken up in exchange with internal P_i (1, 8). Uptake of G3P without P_i exchange is essentially by proton symport. Under these conditions, GlpT-mediated uptake of G3P can serve as the sole source of P_i. The GlpT permease is a tightly membrane-bound oligomeric complex of identical polypeptide subunits (13). G3P can also be taken up by the Ugp (uptake of glycerol phosphate) system. The Ugp system is a typical periplasmic binding protein-dependent multicomponent transport system specific for G3P and glyceryl phosphoryl phosphodiesters, the diacylation products of phospholipids (4, 21). The genes *ugpB*, *ugpA*, *ugpE*, *ugpC*, and *ugpQ* (18) form an operon located at 75 min on the *E. coli* chromosome encoding the specific binding protein (*ugpB*) (2), the two membrane-bound components (*ugpA* and *ugpE*), and the ATP-binding-fold-containing subunit (*ugpC*), which is supposedly the energy module of the system. The *ugp* operon is under the control of PhoB, the central gene activator of the *pho* regulon (3).

The last transport system recognizing G3P is the Uhp system specific for hexose phosphates (12). Since Uhp is not induced in the absence of glucose-6-phosphate, it is not relevant to the phenomena discussed in the present publication and will thus not be considered further.

Some time ago, we observed that when G3P is transported exclusively via the Ugp system (in a *phoA glpT pst* mutant), it can be used as the sole source of P_i but not as the sole source of carbon. In contrast, G3P that is transported exclusively via GlpT (in a *phoA ugp glpR* mutant) can be used as the sole source of carbon and as the sole source of P_i (21). The explanation for the inability of G3P to support growth when transported by Ugp, in spite of high transport activity inherent in Ugp, was the observation that when P_i is allowed to be transported by Pst, it inhibits Ugp-mediated uptake of G3P. Therefore, after being taken up by the Ugp system, G3P during its metabolism would release P_i that would accumulate and inhibit further uptake of G3P (5). G3P that is taken up by the GlpT system would also produce internal P_i but, in contrast to the Ugp system, would release P_i in exchange for the incoming G3P and even stimulate the utilization of G3P. This study did not allow direct determination of the internal P_i concentration after uptake of G3P, and one could argue that a metabolic product of P_i (and thus G3P) could have caused the inhibition of Ugp.

In the present publication, we monitored by ^{31}P-nuclear magnetic resonance (NMR) the concentration of internal P_i after the addition of G3P under conditions in which G3P was transported either by the Ugp or by the GlpT system or by both. In vivo ^{31}P-NMR is an ideal technique for these studies because of its noninvasive characteristics, allowing concentrations of extracellular and intracellular phosphorylated metabolites in a single sample to be monitored. Intracellular concentrations of P_i in the range of 3 to 9 mM have been reported for *E. coli* in the pioneering in vivo NMR studies of Shulman's group (22, 23). We found that internal P_i rises to higher internal levels when G3P is transported by the Ugp system. The increase in internal P_i concentration was not unlimited. It does not exceed a certain maximal level of about 30 mM, and excess

* Corresponding author. Mailing address: Department of Biology, University of Konstanz, D-78434, Konstanz, Germany. Phone: 49 7531 882658. Fax: 49 7531 883356

TABLE 1. Bacterial strains used in this study

Strain[a]	Known genotype	Reference or source
Brz70	F$^-$ Δ(*glpT-glpA*)593 *gyrA phoST*^{b} *ugp*$^+$ *glpD*$^+$ λpSH260$^-$ (*ugpA-lacZ*) *tsx*::Tn*10 phoA8 glpR*	5
Brz80	F$^-$ *phoST*^{b} *glpT*$^+$ *glpD*$^+$ *phoA8 ugpA704*::Tn*10* λp68-1 (*glpT-lacZ*) *glpR*	5
Brz35	F$^-$ Δ(*glpT-glpA*)*593 gyrA phoST*^{b} *glpD2 ugp*$^+$ *tsx*::Tn*10 phoA8 glpR*	5
KM517	F$^-$ *phoST*^{b} *glpT*$^+$ *glpD2 phoA8 ugpA704*::Tn*10* λp68-1(*glpT-lacZ*) *glpR*	This study
Brz503	F$^-$ Δ(*glpT-glpA*)*593 gyrA ugp*$^+$*glpD*$^+$ Δ*phoA20 glpR*	5
HA18	Δ*phoA20*	10
MC4100	F$^-$ *araD* Δ(*argF-lac*)U169 *rpsL150 relA1 deoC1 flbB5301 deoC1 ptsF25 rbsR*	6

[a] All strains are derivatives of strain MC4100 and carry all of its known markers as shown in this table.

[b] Old nomenclature for *pstS* and *pstA*.

P_i is excreted into the medium. In contrast, after the uptake of G3P exclusively by the GlpT system, the initial internal P_i concentration is maintained, despite the production of large amounts of P_i which are rapidly excreted in the medium.

MATERIALS AND METHODS

Bacterial strains and growth conditions. All bacterial strains used are derivatives of *E. coli* K-12 (Table 1). The strains were grown under aeration in G+L (Garen and Levinthal) medium (9) with 0.1 mM P_i as the only phosphate source and with 0.2% glycerol as the carbon source until growth stopped because of the limitation in P_i. In this way, the strains reached an optical density at 578 nm (OD_{578}) of 0.8 to 1.0. In the cases of strains Brz35 and KM517, both of which contain a *glpD* mutation that prevents growth on glycerol, 0.2% maltose instead of glycerol was used as the carbon source. Strain Brz80 was made kanamycin resistant and maltose negative by using P1 grown on a *malT*::Tn*5* strain; KM517 arose by transduction of this strain to a maltose-positive and glycerol-negative phenotype using P1 grown on Brz35 (*glpD*). For the NMR measurements, fresh cultures were prepared for each experiment. Cells were harvested by centrifugation at 7,000 × *g* for 15 min at 4°C and washed twice with 100 mM 2-(*N*-morpholino)ethanesulfonate (MES) buffer (Sigma), pH 6.6, containing 1 mM $MgCl_2$; the cell pellet was resuspended in the same buffer to a final volume of 3.5 ml and a calculated OD_{578} of 60 to 80 and was transferred to a 10-mm NMR tube. D_2O was added to a final concentration of approximately 5% (vol/vol) in order to provide a lock signal.

NMR spectroscopy. ^{31}P-NMR spectra were recorded at 202.4 MHz without proton broad band decoupling using a Bruker AMX500 spectrometer and a 10-mm quadruple-nucleus probe head for detection of ^{31}P, ^{1}H, ^{13}C, and ^{15}N. Typical acquisition parameters were as follows: spectral width, 26.3 kHz; datum size, 16,000; repetition delay, 0.7 s; pulse width, 12 μs (corresponding to a 45° flip angle); number of scans, 124. It was checked that these acquisition conditions allowed full relaxation of the resonance due to internal P_i. Efficient mixing and supply of oxygen to the cell suspension in the NMR tube were achieved by bubbling oxygen and using an airlift system (20), yielding a flow of O_2 in excess of 30 ml/min. To ensure that the cells were properly energized, the steady-state concentration of ATP was measured by NMR and was found to be in the millimolar range. Spectra were run at a probe head temperature of 37°C. Chemical shifts were referenced to the resonance of methylphosphonate (at 30.2 ppm) contained in a capillary tube inserted in the sample NMR tube which was also used for phosphorus quantitation. The internal P_i pool was quantitated by comparing the intensity of the corresponding resonance with that of the methylphosphonate resonance in a spectrum run under nonsaturating conditions (repetition delay, 20 s) at the end of each in vivo NMR experiment. The methylphosphonate capillary was previously calibrated by comparison of the intensity of the methylphosphonate resonance with that of P_i in a solution of this compound with an accurately known concentration. Intracellular and extracellular pH values were determined from the chemical shifts of either P_i or G3P by using calibration curves obtained in the same buffer. In a typical experiment, after acquisition of the initial spectrum, G3P was added to a final concentration of 3.4 mM and ^{31}P-NMR spectra (1.5 min each) were sequentially acquired. Each type of experiment with living cells was repeated at least twice.

Estimation of the internal volume. Cultures of strains Brz70 and Brz80 were grown in G+L medium with 0.1 mM P_i with glycerol as the carbon source as described above. The OD_{578} (0.9 and 0.95), as well as the living cell count (using Luria-Bertani plates), was determined (6.4×10^8/ml and 4.8×10^8/ml). A 200-ml volume of these cultures was filtered through a Millipore filter (pore size, 0.45 μm) and washed with distilled water. The filters were dried at 100°C for 45 min, and their weights were determined. These weights divided by the number of living cells gave values of 0.334×10^{-12} g (dry weight) per cell for strain Brz70 and 0.464×10^{-12} g per cell for Brz80. The dry weight was taken as 30% of the wet weight of living cells, whereas 70% of the wet weight was taken as the internal volume (17). Thus, for the two strains, the relationship of OD_{578} to internal volume is the following: 1 ml of culture exhibiting an OD_{578} of 1 equals internal volumes of 0.61 μl for Brz70 and 0.54 μl for Brz80. Thus, despite the small difference in cell numbers per OD_{578} measurement (slightly different volumes), the mass or the internal volume per OD_{578} measurement is rather constant. For the estimation of the internal volume, for all strains we used the following correlation: OD_{578} of 1 equals an internal volume of 0.6 μl per ml of culture.

Transport of [^{14}C]G3P and $^{32}P_i$. Transport of [^{14}C]G3P and $^{32}P_i$ was done essentially as described previously (5), with cells grown with glycerol as the carbon source and under conditions of either P_i starvation (initially 0.1 mM) or excess P_i (5 mM). *glpD* strains (Brz35 and KM517) were grown with 0.2% maltose as the carbon source. They were washed with and resuspended in G+L medium without P_i. The concentration of [^{14}C]G3P was either 0.7 μM or 1 mM. The initial rate of uptake was determined with cultures at an OD_{578} of 0.5 (in the case of the low substrate concentration) and at an OD_{578} of 5 (in the case of the high substrate concentration).

For measuring $^{32}P_i$ uptake by the Pst system (see Table 4), strains Brz503 and Brz70 were grown in G+L medium with 0.1 mM P_i and maltose as the carbon source. They were resuspended in the same medium without a carbon source and without P_i to an OD_{578} of 0.5. The substrate, trace amounts of $^{32}P_i$, was adjusted with $^{31}P_i$ to 1 μM. G3P (0.1 mM) was added either together with $^{32}P_i$ or 5 min prior to the addition of $^{32}P_i$.

For the $^{32}P_i$ chase experiment (Table 2), strain Brz503 was treated as described above. Cells were exposed for 5 min to 1 μM $^{32}P_i$. Then, either G3P or $^{31}P_i$ (0.1 mM each) was added, and the remaining $^{32}P_i$ content was determined by filtration.

TABLE 2. Chase of internal $^{32}P_i$ by Ugp-mediated uptake of G3P or Pst-mediated uptake of P_i in strain Brz503 (Pst$^+$ Ugp$^+$)[a]

Min after addition of G3P or P_i	Internal $^{32}P_i$ concn (mM)		
	No addition	Addition of 0.1 mM G3P	Addition of 0.1 mM P_i
0	2.92	2.85	2.61
10	2.80	2.63	2.48
20	2.97	2.56	2.14
30	2.64	2.01	1.96
60	2.70	1.23	1.40

[a] Samples were taken after 5 min of exposure of cells to 1 μM $^{32}P_i$, when 86% of the label had been taken up.

RESULTS

P_i accumulates after Ugp-mediated uptake of G3P. Strain Brz503 (*phoA glpT pst*$^+$ *ugp*$^+$) was grown on glycerol initially with 0.1 mM P_i until growth ceased because of P_i limitation, which are conditions that induce the *pho* genes, including the *ugp* operon. The cells were washed and resuspended in MES medium (free of P_i and a carbon source) at a density of 5.7×10^{10} cells per ml, aerated with O_2, and analyzed by ^{31}P-NMR. Extracellular P_i can easily be distinguished from intracellular P_i by ^{31}P-NMR because of the pH dependence of the P_i resonance and the different pHs of extracellular and intracellular compartments. All further NMR measurements were done with cells treated initially in this way. Under the conditions of the experiment, the cells contained initially less than 1 mM internal P_i. G3P (3.4 mM) was added to the washed cell suspension. Concomitant with the decrease of external G3P, internal P_i increased; however, no significant amounts of internal G3P could be detected with this strain (Fig. 1A). After 12 min, internal P_i (13 mM) no longer increased but P_i appeared in the external medium. The internal concentration of P_i leveled off

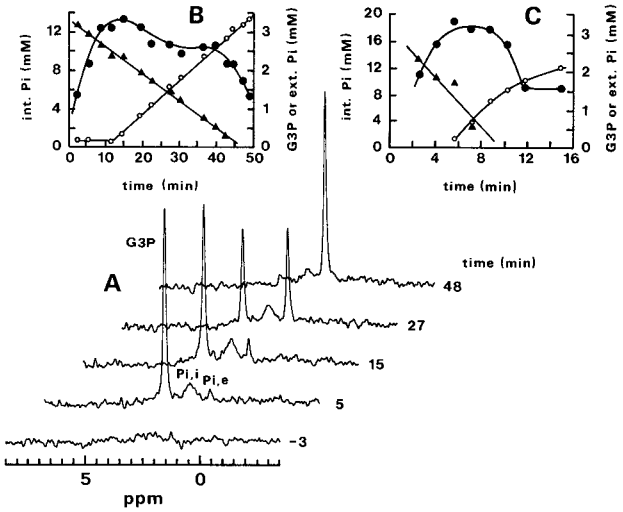

FIG. 1. (A) ^{31}P-NMR spectra of an aerated cell suspension (OD_{578} of 80) of strain Brz503 (*phoA glpT ugp*$^+$ *pst*$^+$) at 37°C. Cells were grown on glycerol initially with 0.1 mM P_i until growth ceased because of P_i limitation. After the acquisition of the first spectrum, G3P (final concentration, 3.4 mM) was added at time zero, and spectra (1.5 min each) were sequentially acquired. The increase in cellular P_i upon G3P metabolism is clear. Resonance assignments: G3P, external G3P; Pi,i, intracellular P_i; Pi,e, external P_i. (B) Time course of the concentrations of external (ext.) G3P (▲), internal (int.) P_i (●), and external P_i (○) as measured by ^{31}P-NMR in the experiment illustrated in panel A. (C) Time course of the concentrations of the same compounds measured in a similar experiment but performed with strain Brz70 (*phoA glpT pst ugp*$^+$).

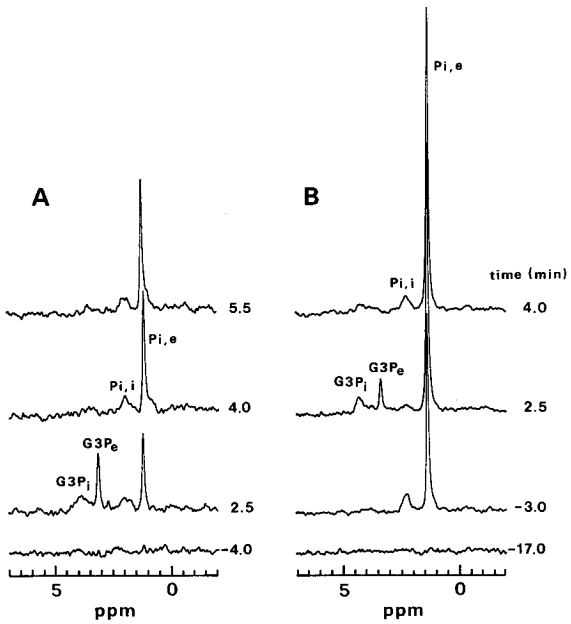

FIG. 2. (A) ^{31}P-NMR spectra of an aerated cell suspension (OD_{578} of 80) of strain HA18 (*phoA ugp*$^+$ *glpT*$^+$ *pst*$^+$) grown on glycerol with 0.1 mM P_i until cessation of growth on account of P_i limitation. G3P (3.4 mM) was added at time zero, and spectra were acquired sequentially at 37°C. (B) 3.4 mM P_i supplied at approximately 15 min before the addition of G3P. Resonance labeling: $G3P_i$, internal G3P; $G3P_e$, external G3P; Pi,i, internal P_i; Pi,e, external P_i.

at about 10 mM as long as external G3P was present, and it declined thereafter (Fig. 1B).

Brz70 (*phoA pst glpT ugp*$^+$) showed qualitatively the same behavior, although the accumulation of internal P_i was higher (19 mM). In addition, the internal P_i concentration leveled off after external G3P was used up (Fig. 1C). Brz70 is constitutive for the *pho* regulon on account of the lack of the Pst transport system. Thus, the accumulation of internal P_i after the addition of G3P in both strains was not due to the reaccumulation of external P_i after its internal formation from G3P, which was followed by its secretion. Rather, it was accumulated internally after its formation from G3P and exited the cell only when the internal level became high (above 13 mM). Surprisingly, it appeared that the absence of Pst, the high-affinity P_i transport system, led to higher internal levels of P_i after its formation from G3P that had been taken up by the Ugp system. The exit of internal P_i after the addition of G3P or P_i to cells of strain Brz503 that had accumulated P_i by the Pst system can also be reproduced by the filtration technique using $^{32}P_i$ as the labeled substrate (Table 2).

When strain HA18 (*phoA ugp*$^+$ *glpT*$^+$ *pst*$^+$) was used in these experiments, the pattern was different (Fig. 2A). In HA18 which was grown under these conditions, both the GlpT and the Ugp transport systems were present and contributed to the uptake of G3P. G3P was very quickly taken up, and at 2.5 min after its addition, internal G3P and P_i could be detected. Apparently, the uptake of G3P is so fast that G3P dehydrogenase cannot keep up with its accumulation. In contrast to strains Brz503 and Brz70 (both of which lack the GlpT system), P_i appeared in the medium already after 2.5 min, the earliest time point. At 4 min after the addition of G3P, external G3P was used up and internal G3P was no longer visible but internal P_i had accumulated (13 mM). When HA18 which was grown under the same conditions was first preincubated with 3.4 mM P_i and then exposed to G3P, the accumulated internal P_i concentration dropped temporarily from 8.0 to 3.5 and internal G3P appeared. Again, after external G3P had been used up, internal G3P disappeared and internal P_i was high (Fig. 2B). From the behavior of internal P_i, it is clear that G3P transported in strain HA18 under conditions depicted in the legend to Fig. 2A (low internal P_i) is mainly mediated by Ugp, whereas under the conditions depicted in the legend to Fig. 2B (high internal P_i), it is mediated preferentially by GlpT.

P_i does not accumulate when G3P is taken up exclusively by the GlpT system. Strain Brz80 (*phoA pst ugp glpR glpT*$^+$) was grown on glycerol initially with 0.1 mM P_i until growth ceased on account of P_i limitation. Since the strain was grown on glycerol and was in addition *glpR*, the cells expressed the *glp* regulon, including the GlpT transport system, at a high level. After the addition of G3P, no accumulation of either G3P or P_i could be detected. Uptake of G3P was slow and P_i appeared in the medium at 6 min after the addition of G3P (Fig. 3A).

The addition of 3.4 mM P_i to Brz80 (*phoA pst ugp glpR glpT*$^+$), which was grown and treated under the conditions described above, led to the accumulation of internal P_i (about 10 mM). The further addition of G3P led to the fast disappearance of external G3P. Internal G3P could not be detected, and the internal P_i concentration increased to 14 mM after external G3P had been used up (Fig. 3B and C). Note that the rate by which G3P was taken up in the presence of internal P_i (Fig. 3B) was about twofold higher than that in the absence of internal P_i (Fig. 3A). During the uptake of G3P, excess P_i derived from the metabolized G3P was secreted into the medium without altering the internal concentration of P_i. During the GlpT-mediated uptake of G3P in the presence of high internal P_i, we noticed that the internal pH rapidly and temporarily increased from 7.3 to 7.7, as seen by the shift of the internal P_i peak (Fig. 3B).

Steady-state accumulation of P_i after Pst-mediated transport of P_i followed by Ugp-mediated uptake of G3P. Strain

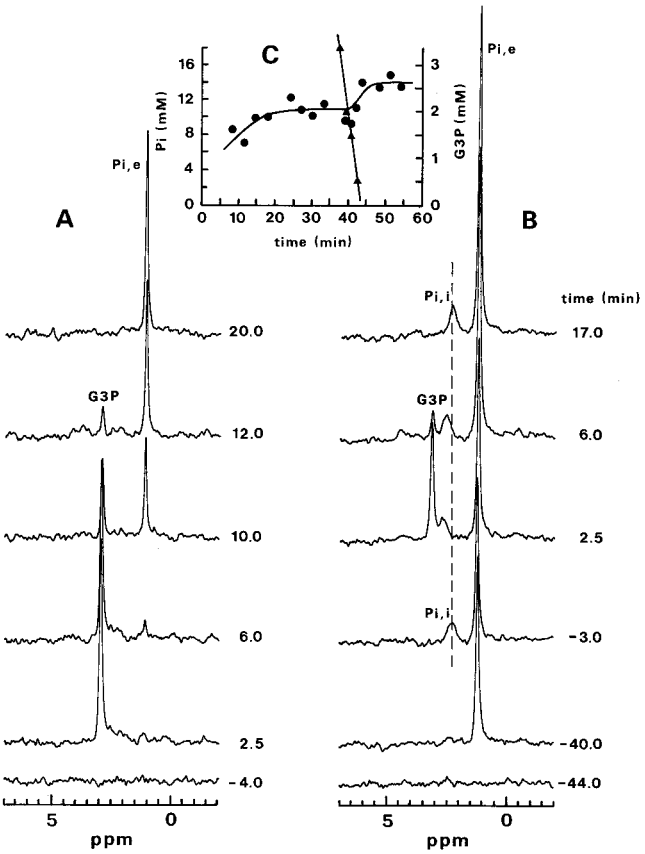

FIG. 3. (A) ^{31}P-NMR spectra of an aerated cell suspension (OD_{578} of 85) of strain Brz80 (*phoA ugp pst glpR glpT*$^+$) grown on glycerol with 0.1 mM P_i until cessation of growth on account of P_i limitation. G3P (3.4 mM) was added at time zero, and spectra were acquired sequentially at 37°C. (B) 3.4 mM P_i supplied approximately 40 min before the addition of G3P. In this case, the alkalinization of the cytoplasm upon G3P metabolism is apparent from the shift of the internal P_i resonance to higher frequency. Resonance labeling is as described in the legend to Fig. 1. (C) Time course of the concentrations of external G3P (▲) and internal P_i (●) as measured by ^{31}P-NMR in the experiment illustrated in panel B.

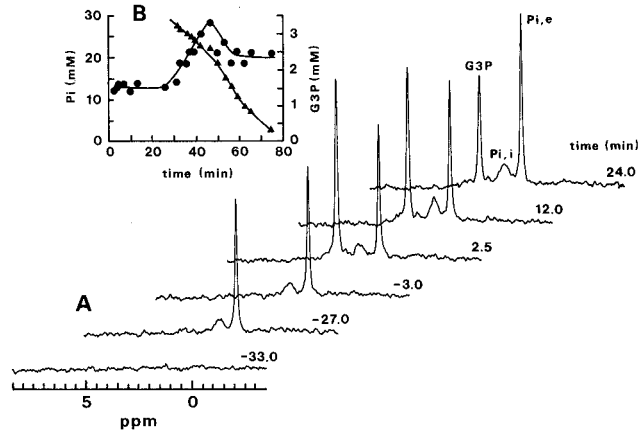

FIG. 4. (A) ^{31}P-NMR spectra of an aerated cell suspension (OD_{578} of 80) of strain Brz503 (*phoA glpT ugp*$^+$ *pst*$^+$) at 37°C. Cells were grown on glycerol initially with 0.1 mM P_i until growth ceased because of P_i limitation. After the acquisition of the first spectrum, 3.4 mM P_i was added and spectra were acquired sequentially in order to monitor the accumulation of internal P_i. G3P (3.4 mM) was added at time zero (approximately 30 min after the P_i addition), and spectra (1.5 min each) were sequentially acquired. (B) Time course of the concentrations of external G3P (▲) and internal P_i (●) as measured by ^{31}P-NMR in the experiment illustrated in panel A. Labeling of resonances is as described in the legend to Fig. 1.

Brz503 (*phoA glpT ugp*$^+$ *pst*$^+$) was grown on glycerol initially with 0.1 mM P_i until growth ceased on account of P_i limitation, conditions that induce the *pho* genes, including the *pst* operon. P_i (3.4 mM) was added. Internal P_i rapidly accumulated to about 13 mM and remained constant thereafter. After the addition of G3P, it was slowly taken up, and the internal P_i concentration rose to nearly 30 mM before it leveled off at about 20 mM (Fig. 4).

Uptake of G3P in *glpD* strains. Strain Brz35 (*phoA pst glpT glpD ugp*$^+$) was grown on maltose with 0.1 mM P_i until growth ceased on account of P_i limitation. In addition, the cells were *glpD* and therefore unable to oxidize G3P to dihydroxyacetone. The addition of G3P led to the rapid accumulation of internal G3P, which was followed by it slow metabolism, accumulation of internal P_i, and excretion of P_i into the medium (Fig. 5A).

When strain KM517 (*phoA pst ugp glpR glpD glpT*$^+$) was used under the same experimental conditions, G3P was also taken up. Internal P_i did not accumulate at first, but P_i immediately appeared in the medium. Again, G3P accumulated but was slowly degraded. After external G3P was used up, internal P_i accumulated (Fig. 5B). Apparently, the *glpD* mutation is leaky, allowing slow oxidation of G3P to dihydroxyacetone. In addition, it is clear that even in the absence of the high-affinity Pst transport system, P_i can enter cell, as is shown by the decrease in the intensity of the external P_i peak in the three top spectra of Fig. 5B. When G3P was added to cells that had been preloaded with P_i, internal P_i was immediately drained while G3P accumulated (data not shown).

Transport activities for G3P mediated by Ugp or GlpT after growth at low or high external P_i. Measurements for the rate of uptake by ^{31}P-NMR are rather slow in comparison to the filter technique using radioactively labeled compounds. Since it became obvious that the uptake of G3P by the Ugp and the GlpT systems was in an inverse fashion very sensitive to internal P_i and since both systems had originally been compared under identical conditions (21), we measured the uptake of G3P under conditions that are optimal for the two systems. Table 3 summarizes transport assays using [^{14}C]G3P in strains that transport G3P either by the GlpT or the Ugp system. In each case, the respective transport system is fully induced. The bacterial cultures were assayed in G+L medium in the absence of external P_i after they had been grown either at high or low external P_i. Despite the washings with P_i-free medium, the internal P_i concentration remained high (about 10 mM) when the cells were grown at high (5 mM) P_i concentrations. They were below 1 mM when the cells were grown at limiting P_i concentrations. All strains were *pst* and therefore constitutive for the *pho* regulon, including the Ugp system. Two substrate concentrations, 0.7 μM and 1 mM, were used. At the low substrate concentration of 0.7 μM, the Ugp system would be more effective because of its low K_m; at the high concentration of 1 mM, both systems would be operating at their maximum rates. As can be seen in Table 3, the internal P_i concentration had a profound influence on the ability to take up G3P via the two systems. Whereas the GlpT system was stimulated at a high internal P_i concentration, the Ugp system was inhibited. When it was measured at a 1 mM substrate concentration in strains that could metabolize G3P and under their respective optimal conditions, the V_{max} (maximum rate of transport) of the GlpT system was 5.7 times faster than that of the Ugp system (81 versus 14 nmol/min/10^9 cells). On the other hand, at

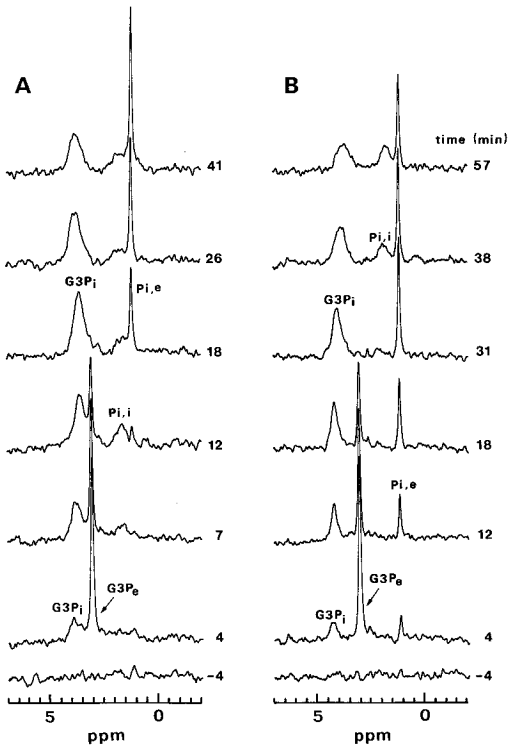

FIG. 5. ^{31}P-NMR spectra of aerated cell suspensions of two *glpD* strains at 37°C. (A) Brz35 (*phoA glpT glpD pst ugp*$^+$); (B) KM517 (*phoA ugp glpD pst glpT*$^+$). Cells were grown on maltose with 0.1 mM P_i until cessation of growth because of P_i limitations. At time zero, 3.4 mM G3P was added and spectra were sequentially acquired. Resonance labeling is as described in the legend to Fig. 2.

a concentration of 0.7 μM, the Ugp system was twice as effective as the GlpT system (0.8 versus 0.4 nmol/min/10^9 cells).

P_i uptake by the Pst system is not inhibited by a high concentration of internal P_i. Since we observed inhibition of Ugp-mediated G3P uptake by internal P_i, it seemed reasonable that the Pst-mediated uptake of P_i could also be inhibited in the presence of high internal P_i concentrations. Therefore, for strain Brz503 after growth in G+L medium and with 0.1 mM P_i (derepression of Ugp and Pst) we tested the ability of unlabeled G3P that entered the cells by the Ugp system (and that metabolized internally to P_i) to inhibit the Pst-mediated uptake of $^{32}P_i$. Table 4 demonstrates that the initial rate of uptake in the presence of G3P with or without a 5-min incubation (and therefore internal production of P_i) is the same. This indicates that Pst is not controlled in its activity by internal P_i. The presence of G3P appears to inhibit by about 30% the uptake of $^{32}P_i$. This is probably due to a small contamination of G3P with P_i, since the observed inhibition is not time dependent.

DISCUSSION

The Ugp and the GlpT transport systems, both of which can transport G3P against the concentration gradient, are well adapted to the two different physiological situations that *E. coli* may encounter. One is phosphate starvation; the other is the availability of glycerol and glycerol-containing compounds as a carbon source. The response occurs on two levels. One is on the level of gene expression; the other is on the level of transport activity. This second level is the subject to the present publication. By using ^{31}P-NMR, we found that when G3P is transported by the P_i starvation-inducible Ugp system, it will always lead to an increase in the internal P_i concentration, provided that G3P can be metabolized. This is true regardless of whether the G3P-inducible GlpT system is present and whether G3P is transported by it. G3P will not accumulate; however, its metabolism will produce internal P_i. The accumulating internal P_i will then inhibit further uptake of G3P by the Ugp system. We previously had observed the inhibition of G3P uptake when P_i uptake via the Pst system was allowed (5), suggesting that it was internal P_i that inhibited the Ugp transport system from inside. That study did not allow direct measurement of internal P_i concentration. Here, we demonstrate that the uptake of G3P via the Ugp system in a strain allowing G3P metabolism is always accompanied by an increase in the concentration of internal P_i (Fig. 2) that is paralleled by the inhibition of Ugp-mediated G3P transport (Table 3). However, it is clear that even the highest observed internal P_i concentration of about 30 mM is not sufficient to completely prevent the uptake of G3P by the Ugp system (Fig. 4).

An important conclusion from our study is the observation that internal P_i will never accumulate to more than 30 mM, even under conditions in which G3P continues to be pumped into the cell and is metabolized to P_i. The production of excess P_i leads to the secretion of P_i into the medium. It seems that the secretion starts only when a threshold value of internal P_i (about 13 mM) is reached. So far, it is entirely unclear how this secretion of P_i occurs. Preliminary results (data not shown) indicated that the Pit transport system (7) does not mediate the exit of P_i.

In contrast to the uptake of G3P by the Ugp system, the uptake of G3P by the GlpT system does not lead to the accumulation of internal P_i as long as G3P can be metabolized. Only in the presence of high concentrations of internal P_i is the uptake of G3P so fast that its internal presence can be seen temporarily (Fig. 2). The observation that the internal P_i concentration does not increase during the uptake of G3P can be

TABLE 3. Initial rate of transport of G3P by the Ugp or the GlpT system after growth in the presence of low or high P_i[a]

Strain	Rate of transport (nmol/min/10^9 cells)			
	Growth with 5 mM P_i		Growth with 0.1 mM P_i	
	0.7 μM G3P	1 mM G3P	0.7 μM G3P	1 mM G3P
KM517 (GlpT$^+$ GlpD$^-$)	0.98	105	0.27	5.5
Brz80 (GlpT$^+$ GlpD$^+$)	0.44	81	0.04	5.2
Brz35 (Ugp$^+$ GlpD$^-$)	0.14	2.8	0.98	6.8
Brz70 (Ugp$^+$ GlpD$^+$)	0.37	0.82	6.4	14.17

[a] Cells were grown in G+L medium in the presence of 0.1 or 5 mM P_i overnight. They were washed and resuspended in G+L medium without P_i. G3P transport was performed with 0.7 μM or with 1 mM [^{14}C]G3P as the substrate at room temperature.

TABLE 4. Effect of Ugp-mediated uptake of G3P on the initial rate of Pst-mediated P_i uptake[a]

Strain	$^{32}P_i$ uptake (nmol/min/10^9 cells)[a]		
	No additions	0.1 mM G3P	5-min preincubation with 0.1 mM G3P
Brz503 (Pst$^+$ Ugp$^+$)	3.4	2.8	2.8
Brz70 (Pst$^-$ Ugp$^+$)	0.03	0.05	0.04

[a] $^{32}P_i$ uptake was measured at a 1 μM concentration. Values were measured at room temperature.

explained by the stoichiometric exchange between G3P coming in and P_i coming out and both being mediated by the same system (1, 8). The rate by which G3P is taken up by the GlpT system depends strongly on the internal P_i concentration. This is seen by the uptake experiments shown in Table 3 and by the NMR experiments shown in Fig. 3. At high internal P_i concentrations, the fast entry of G3P leads to a shift toward a higher pH that cannot be seen when the internal P_i concentration is low (Fig. 3). We interpret this alkalization at high internal P_i concentration as caused by an increase in the rate of G3P oxidation and hence increased extrusion of protons.

Only when P_i has been secreted into the medium in appreciable amounts does the internal P_i concentration begin to rise, apparently because of the uptake of external P_i.

The situation is different when G3P uptake by the GlpT system is monitored in a *glpD* mutant strain that is defective in the oxidation of G3P. In such a strain, G3P is accumulated and no internal P_i can be detected at first. The *glpD* mutation appears to be leaky, since the internal G3P concentration slowly declines and P_i appears in the external medium. Only when the external G3P concentration becomes low and external P_i increases does internal P_i concentration increase as well (Fig. 5B). When G3P uptake via the Ugp system is monitored in a *glpD* mutant strain, the internal P_i concentration is not reduced but slowly increases on account of the slow metabolism of G3P (leakiness of the *glpD* mutation) (Fig. 5A).

Our experiments allow a description of the events following the uptake of G3P in *E. coli* as it depends on its nutritional environment. Wild-type cells, such as HA18 (Fig. 2), that are starved for P_i will induce the genes of the *pho* regulon including *pst* and *ugp*. When they encounter G3P in the medium, they will take it up via the Ugp system and internal P_i will increase. This in turn will inhibit the Ugp activity and slow down further uptake of G3P. If enough external G3P is present, the internal P_i concentration will continue to rise until a critical level of about 13 mM is reached, upon which P_i is secreted. External P_i will then be recognized by the Pst system, and this will eventually lead to the repression of the entire *pho* regulon (24). Simultaneously, internal G3P will induce the *glp* regulon and G3P will start to enter the cell by the GlpT system. High levels of internal P_i will further stimulate the uptake of G3P via the GlpT system without draining the cell of P_i. The massive exit of P_i (derived from the metabolism of G3P) will further repress the *pho* regulon. Studying the repression of the *pho* regulon by G3P, Rao et al. came to the conclusion that it is not internal but external P_i, after metabolism of internal G3P, that is responsible for repression (19).

In contrast to the study of Rao et al. (19), we show that, depending on the state of induction of the two G3P transport systems and the ability of the strain to metabolize G3P, the internal P_i concentration is not homeostatic. Obviously, there is an upper level for internal P_i concentration. With our estimate of internal cell volume, we conclude that the maximum level is about 30 mM. However, lower values are equally tolerated and will depend on the presence of P_i-containing compounds in the medium. P_i-starved, aerated cells can maintain less than 1 mM P_i. Internal P_i concentration is a function of external P_i, its uptake being mediated by the high-affinity Pst system or the constitutive Pit system. When G3P is the only P_i source, internal P_i will mainly be determined by the Ugp system, whereas the GlpT system preferentially operates as a stoichiometric exchange system, balancing the P_i account.

ACKNOWLEDGMENTS

This study was supported by the Deutsche Forschungsgemeinschaft (SFB156), the Deutsche Akademische Austauschdienst, and the Fond der Chemischen Industrie.

REFERENCES

1. **Ambudkar, S. V., T. H. Larson, and P. C. Maloney.** 1986. Reconstitution of sugar phosphate transport systems of *Escherichia coli*. J. Biol. Chem. **261:** 9083–9086.
2. **Argast, M., and W. Boos.** 1979. Purification and properties of sn-glycerol 3-phosphate-binding protein of *Escherichia coli*. J. Biol. Chem. **254:**10931–10935.
3. **Argast, M., and W. Boos.** 1980. Co-regulation in *Escherichia coli* of a novel transport system for *sn*-glycerol-3-phosphate and outer membrane protein Ic (e,E) with alkaline phosphatase and phosphate-binding protein. J. Bacteriol. **143:**142–150.
4. **Argast, M., D. Ludtke, T. J. Silhavy, and W. Boos.** 1978. A second transport system for *sn*-glycerol-3-phosphate in *Escherichia coli*. J. Bacteriol. **136:**1070–1083.
5. **Brzoska, P., M. Rimmele, K. Brzostek, and W. Boos.** 1994. The *pho* regulon-dependent Ugp uptake system for glycerol-3-phosphate in *Escherichia coli* is *trans* inhibited by P_i. J. Bacteriol. **176:**15–20.
6. **Casadaban, M. J.** 1976. Transposition and fusion of the *lac* genes to selected promoters in *Escherichia coli* using bacteriophage lambda and Mu. J. Mol. Biol. **104:**541–555.
7. **Elvin, C. M., N. E. Dixon, and H. Rosenberg.** 1986. Molecular cloning of the phosphate (inorganic) transport (*pit*) gene of *Escherichia coli* K12; identification of the pit^+ gene product and physical mapping of the *pit-gor* region of the chromosome. Mol. Gen. Genet. **204:**477–484.
8. **Elvin, C. M., C. M. Hardy, and H. Rosenberg.** 1985. P_i exchange mediated by the GlpT-dependent *sn*-glycerol-3-phosphate transport system in *Escherichia coli*. J. Bacteriol. **161:**1054–1058.
9. **Garen, A., and C. Levinthal.** 1960. A fine-structure genetic and chemical study of the enzyme alkaline phosphatase of *Escherichia coli*. Biochim. Biophys. Acta **38:**470–483.
10. **Hartmann, A., and W. Boos.** 1993. Mutations in *phoB*, the positive gene activator of the *pho* regulon in *Escherichia coli*, affect the carbohydrate phenotype on MacConkey indicator plates. Res. Microbiol. **144:**285–293.
11. **Hayashi, S., J. P. Koch, and E. C. C. Lin.** 1964. Active transport of L-alpha-glycerophosphate in *Escherichia coli*. J. Biol. Chem. **239:**3098–3105.
12. **Kadner, R. J., C. A. Webber, and M. D. Island.** 1993. The family of organophosphate transport proteins includes a transmembrane regulatory protein. J. Bioenerg. Biomembr. **25:**637–645.
13. **Larson, T. J., G. Schumacher, and W. Boos.** 1982. Identification of the *glpT*-encoded *sn*-glycerol-3-phosphate permease of *Escherichia coli*, an oligomeric integral membrane protein. J. Bacteriol. **152:**1008–1021.
14. **Larson, T. J., S. Ye, D. L. Weissenborn, H. J. Hoffmann, and H. Schweizer.** 1987. Purification and characterization of the repressor for the *sn*-glycerol 3-phosphate regulon of *Escherichia coli*. J. Biol. Chem. **262:**15869–15874.
15. **Lin, E. C. C.** 1987. Dissimilatory pathways for sugars, polyols, and carboxylates, p. 244–284. *In* F. C. Neidhardt, J. L. Ingraham, K. B. Low, B. Magasanik, M. Schaechter, and H. E. Umbarger (ed.), *Escherichia coli* and *Salmonella typhimurium*: cellular and molecular biology. American Society for Microbiology, Washington, D.C.
16. **Lin, E. C. C., and S. Iuchi.** 1991. Regulation of gene expression in fermentative and respiratory systems in *Escherichia coli* and related bacteria. Annu. Rev. Genet. **25:**361–387.
17. **Neidhardt, F. C.** 1987. Chemical composition of *Escherichia coli*, p. 3–6. *In* F. C. Neidhardt, J. L. Ingraham, K. B. Low, B. Magasanik, M. Schaechter, and H. E. Umbarger (ed.), *Escherichia coli* and *Salmonella typhimurium*; cellular and molecular biology. American Society for Microbiology, Washington, D.C.
18. **Overduin, P., W. Boos, and J. Tommassen.** 1988. Nucleotide sequence of the *ugp* genes of *Escherichia coli* K-12: homology to the maltose system. Mol. Microbiol. **2:**767–775.
19. **Rao, N. N., M. F. Roberts, A. Torriani, and J. Yashphe.** 1993. Effect of *glpT* and *glpD* mutations on expression of the *phoA* gene in *Escherichia coli*. J. Bacteriol. **175:**74–79.
20. **Santos, H., and D. L. Turner.** 1986. Characterization of the improved sensitivity obtained using a flow method for oxygenation and mixing cell suspension in NMR. J. Magn. Reson. **68:**345–349.
21. **Schweizer, H., M. Argast, and W. Boos.** 1982. Characteristics of a binding protein-dependent transport system for *sn*-glycerol-3-phosphate in *Escherichia coli* that is part of the *pho* regulon. J. Bacteriol. **150:**1154–1163.
22. **Ugurbil, K., H. Rottenberg, P. Glynn, and R. G. Shulman.** 1978. ^{31}P nuclear magnetic resonance studies of bioenergetics and glycolysis in anaerobic *Escherichia coli* cells. Proc. Natl. Acad. Sci. USA **75:**2244–2248.
23. **Ugurbil, K., H. Rottenberg, P. Glynn, and R. G. Shulman.** 1982. Phosphorus-31 nuclear magnetic resonance studies of bioenergetics in wild-type and adenosinetriphosphatase(-1) *Escherichia coli* cells. Biochemistry **21:**1068–1075.
24. **Wanner, B. L.** 1993. Gene regulation by phosphate in enteric bacteria. J. Cell. Biochem. **51:**47–54.